Article

Coupled Biohydrogen Production and Bio-Nanocatalysis for Dual Energy from Cellulose: Towards Cellulosic Waste Up-Conversion into Biofuels

Jaime Gomez-Bolivar [1,*,†], Rafael L. Orozco [2,3,†], Alan J. Stephen [2,3], Iryna P. Mikheenko [2], Gary A. Leeke [3], Mohamed L. Merroun [1] and Lynne E. Macaskie [2]

1   Department of Microbiology, Faculty of Sciences, University of Granada, Campus Fuentenueva, 18071 Granada, Spain; merroun@ugr.es
2   Schools of Biosciences, University of Birmingham, Edgbaston, Birmingham B15 2TT, UK; r.l.orozco@bham.ac.uk (R.L.O.); alanste1992@gmail.com (A.J.S.); i.mikheenko@bham.ac.uk (I.P.M.); l.e.macaskie@bham.ac.uk (L.E.M.)
3   Chemical Engineering, University of Birmingham, Edgbaston, Birmingham B15 2TT, UK; g.a.leeke@bham.ac.uk
*   Correspondence: jagobo@ugr.es
†   These authors contributed equally to this work.

Abstract: Hydrogen, an emergent alternative energy vector to fossil fuels, can be produced sustainably by fermentation of cellulose following hydrolysis. Fermentation feedstock was produced hydrolytically using hot compressed water. The addition of CO_2 enhanced hydrolysis by ~26% between 240 and 260 °C with comparable hydrolysis products as obtained under N_2 but at a 10 °C lower temperature. Co-production of inhibitory 5-hydromethyl furfural was mitigated via activated carbon sorption, facilitating fermentative biohydrogen production from the hydrolysate by *Escherichia coli*. Post-fermentation *E. coli* cells were recycled to biomanufacture supported Pd/Ru nanocatalyst to up-convert liquid-extracted 5-HMF to 2,5-dimethyl furan, a precursor of 'drop in' liquid fuel, in a one-pot reaction. This side stream up-valorisation mitigates against the high 'parasitic' energy demand of cellulose bioenergy, potentially increasing process viability via the coupled generation of two biofuels. This is discussed with respect to example data obtained via a hydrogen biotechnology with catalytic side stream up-conversion from cellulose feedstock.

Keywords: biohydrogen; cellulose; hot compressed water hydrolysis; 5-hydroxymethyl furfural up-valorisation; 2,5-dimethyl furan; liquid fuel

1. Introduction

More than 80% of global energy demand is still met via fossil fuels [1]. Hydrogen, emergent for clean transport [2,3], is also widely used in the bulk and fine chemicals sectors, with between 6 and 15% growth annually [4]. Hydrogen production is currently mainly from fossil resources. For some 'clean' applications (e.g., in proton exchange membrane fuel cells (FCs)), petrochemical-H_2 requires purification, whereas 'clean' H_2 produced via fermentation of sugary and waste feedstocks (bio-H_2) can supply a fuel cell directly [5].

Cellulose is one of the most abundant polysaccharides on earth. For efficient utilisation as a source of biofuels, biogases and chemicals its breakdown to smaller monomeric units (glucose) is required through hydrolysis. Cellulose comprises β-(1,4)-linked glucosyl units in water-insoluble crystalline structures which are hard to hydrolyse; hence, the enzymatic breakdown of cellulose to fermentable sugars is slow [6]. It can be accelerated by using 'designer' enzymes, but this requires a high enzyme dosage while enzymatic hydrolysis remains slow [7,8]. A novel protein acted synergistically with cellulases [9]; however, protein purification is costly.

More traditional approaches, e.g., acid hydrolysis, yield glucose at up to 100%, but drawbacks include the corrosion of equipment, a requirement for H_2SO_4 and product recovery from acidic residues [10,11]. A clean alternative, ohmic heating (OH), has been used for hydrolysis (see Supplementary Materials); the advantages include rapid heating and instant shutdown, but disadvantages include 'hot' and 'cold' spots (problematic at scale), with the need to adjust the set-up according to the conductivity of the target liquid.

A more benign approach uses hot compressed water (HCW) at sub-critical temperatures (180 to 300 °C), which enables the solvolysis of cellulose and other complex polysaccharides, such as hemicelluloses and starch [12–14]. For example, Minowa et al. [15] used HCW (200 to 350 °C) with short reaction times using Ni^{2+} or alkali (Na_2CO_3) catalysts. With the former, cellulose decomposition produced little glucose; moreover, a Ni-contaminated hydrolysate would give problems of final waste disposal. Carbonate-catalysis gave a maximum glucose yield at 260 °C; later work confirmed that CO_2 accelerated polysaccharide hydrolysis [16]. Additionally, the diversity of chemical composition of (ligno)cellulosic feedstock itself can have a significant effect on the rate of reaction for other innovative processes, such as aqueous phase (AP) reforming [17]. Modifications in reaction temperatures in AP reforming also favoured hydrogen production when using glucose and xylose as representative compounds of hemicellulose [18]. In the case of HCW, decreasing temperature (to 2 °C/min) increased the glucose yield [13], although toxic degradation by-products were also favoured (e.g., 5-hydroxymethyl furfural: 5-HMF). Despite this, HCW remains the potentially most cost-effective hydrolysis pre-treatment for cellulosic biomass, with the lowest environmental impact [12–14,19].

For the onward fermentation of cellulose hydrolysate, 5-HMF, a potent metabolic inhibitor [20], must be removed, e.g., via use of activated carbon (AC). The efficacy of this was shown in the selective removal of degradation products from starch hydrolysate [21–24]. Hence, AC was initially used in this study to evaluate bio-H_2 synthesis from native and 'cleaned' cellulose hydrolysates.

However, the AC method may not be convenient for 5-HMF side stream valorisation e.g., to 2,5 dimethylfuran (DMF). Here, an effective segregation of 5-HMF from the 'raw' hydrolysate is required as the first step towards biofuel process integration. A liquid/liquid extraction method for 5-HMF extraction was developed (permitting downstream direct addition of catalyst for a one-pot system) taking advantage of the favorable partition coefficient of 5-HMF [25]. Effective solvent extraction of 5-HMF from cellulose hydrolysate into methyl tetrahydrofuran (MTHF; a solvent which can itself be derived from biomass hydrolysate) has been reported previously [26]. MTHF is advantageous due to its low solubility in water while exhibiting similar properties to other widely used alternatives (e.g., tetrahydrofuran; THF) in several organometallic-catalysed reactions [25–27].

Working towards a positive energy balance, obtained from the catalytic hydrogenation of 5-HMF, can be used as a 'drop in' fuel for conventional engines, containing comparable energy to gasoline [28] (energy contents of DMF and gasoline are 31.5 MJ/L and 35 MJ/L, respectively) and bringing the potential to power a local generator, allowing the recycling of energy into the process.

5-HMF, the source of DMF, arises from the dehydration of fructose (and to a lesser extent glucose) catalysed by mineral acids and metal catalysts [29,30]. Biomass contains a significant amount of iron as well as trace transition metals. Hence, the co-production of 5-HMF during hydrolysis of plant cellulose is expected. This, if managed correctly, could potentially deliver dual carbon-neutral energy (i.e., the fermentative bio-H_2 stream (see later) plus the derived DMF component) from cellulosic wastes.

For up-valorisation of the 5-HMF side stream into DMF, a metallic catalyst can be biomanufactured as an alternative to costly commercial catalysts. A one-step conversion (94%) of 5-HMF to DMF using 5 wt% palladium on a carbon commercial catalyst was shown, with 33% yield [31], whereas a comparably active supported Pd-catalyst was made on 'second life' bacterial cells [32–34] (fermentation bio-waste) [32]. The high cost of

catalytic metal was mitigated by metal biorefining from wastes [33,34], which was shown as economically feasible by an example Life Cycle Analysis [35].

With respect to the fermentation as a source of waste bacteria, various microbial systems have been used for bio-H_2 production [36]. *E. coli*, while not necessarily the best for industrial application, has well-defined molecular genetic tools to optimise metabolic pathways. It is important to note that while the disposal of genetically modified organisms is problematic, the metallisation process kills the cells. *E. coli* cells left over from the biohydrogen fermentation (below) were used ('second life') to make a supported 'bio-Pd' catalyst, which had comparable activity to commercial comparators [32,37]. Later work showed that a bio-Pd/Ru bimetallic catalyst was active in 5-HMF up-conversion to DMF using *Bacillus benzeovorans* [38] and *Desulfovibrio desulfuricans* [27]. Bio-Pd/Ru was used in this study using *D. desulfuricans* in comparison to post-fermentation *E. coli* cells for catalyst fabrication, following the liquid–liquid extraction for 'one-pot' 5-HMF separation from the fermentation liquor and its catalytic upgrading.

The potential viability of a biorefinery approach for a dual product stream is limited by hydrogen production. For the *E. coli* dark fermentation (DF) this is (via an irreversible reaction) maximally 2 mols H_2 per mol glucose (see [39,40]), which maintains sufficient partial pressure of H_2 to drive a fuel cell directly [5]. Higher H_2 yields can be achieved (but via a reversible reaction) using other microorganisms. However, this self-limits the H_2-partial pressure (discussed in [41]). As an alternative, a secondary photo-fermentation (PF) of the aqueous DF stream increases the hydrogen yield by several-fold. The PF converts the organic acids (OA) fermentation co-products of *E. coli* into a second biohydrogen stream [39–41]. This method employs the electrodialytic extraction of OAs into a coupled DF/PF 'biohydrogen from waste' system, which outperformed other sustainable technologies [39,40], but with no comparable energy balances were made. In this integrated system, the DF/PF would be further value-added by catalytically upgrading in parallel the hydrolysis side stream into a liquid biofuel precursor as we describe in the current study, the overall goal being to estimate the overall energy balance using obtained data from cellulose to underpin a future Life Cycle Analysis (LCA) and economic assessment, which would also factor-in the additional benefits of carbon mitigation and waste minimisation, which, along with circularity, do not feature in standard LCAs. The integration of fermentation (bio-H_2) and parallel chemical catalysis (for DMF production) would also realise additional benefits, which include mitigation of waste disposal costs (i.e., used bacteria and the hydrolysis side-stream), while realising resources from waste, working towards process circularity, especially since fermentation waste CO_2 has the potential to be recycled into catalysing cellulose hydrolysis upstream (see above). Onward assessments would also consider the value of the 'saved' carbon (EU emission trading value of carbon is \$50/t June 2021; Source Carbonpricingdashboard.worldbank.org, accessed on 23 January 2022).

The hypothesis driving this study is that a positive energy balance can be achieved by the integration of the component chemical and biotechnologies and the specific objective is to prove or disprove this hypothesis.

The overall goal of this program is energy efficient waste conversion via integrated bio-H_2 and 2,5 DMF generation, the aim of this study being to examine a model cellulose HCW hydrolysate suitable for, and utilised into, parallel downstream valorisations: (i) dark and photo-fermentations to produce bio-H_2 (after 5-HMF removal) and (ii) catalytic up-conversion of harvested 5-HMF into 2,5 dimethylfuran (DMF). The 'parasitic' energy demand is mainly driven by the energy consumed in the HCW hydrolysis and in the hydrogenation reaction of 5-HMF into 2,5 DMF, underpinning the objective—to assess whether a positive energy balance is (or could become) feasible.

2. Results and Discussion

2.1. Hydrolysate Production, Detoxification, and Fermentation into Biohydrogen by E. coli

2.1.1. Cellulose Hydrolysis under N_2 and CO_2 Using Hot Compressed Water and Preparation of Hydrolysate

The thermal pathways from 220–260 °C (58 to 80 bar) are shown in Figure 1. The heating rate (~7 °C/min) exceeded the minimum 2 °C/min required for maximum sugar yields [13,42].
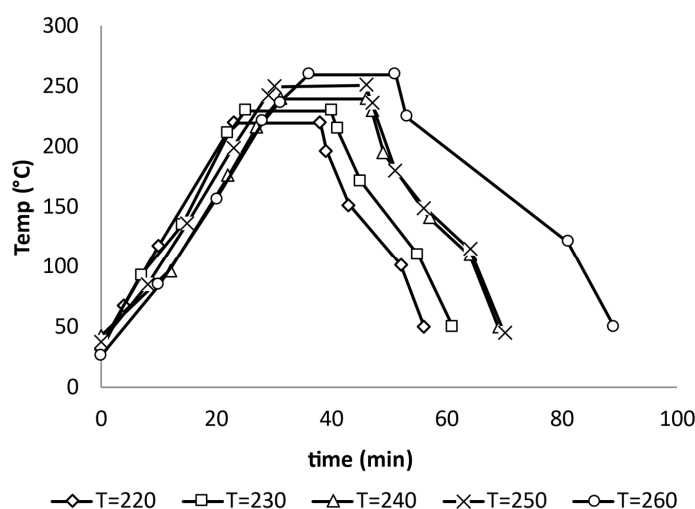

Figure 1. Reaction heating and cooling pathways delivered by the reactor at different temperatures. There was no difference between tests using CO_2 and N_2. Set temperatures (°C) were: ◇, 220; □, 230; △, 240; X, 250; O, 260. Heating pathway is based on average values from two experiments, with variation between replicates within ±5%.

The conversion of cellulose (X_c, %) into products under N_2 and CO_2 is shown in Figure 2a,b, respectively, increasing exponentially with respect to temperature.
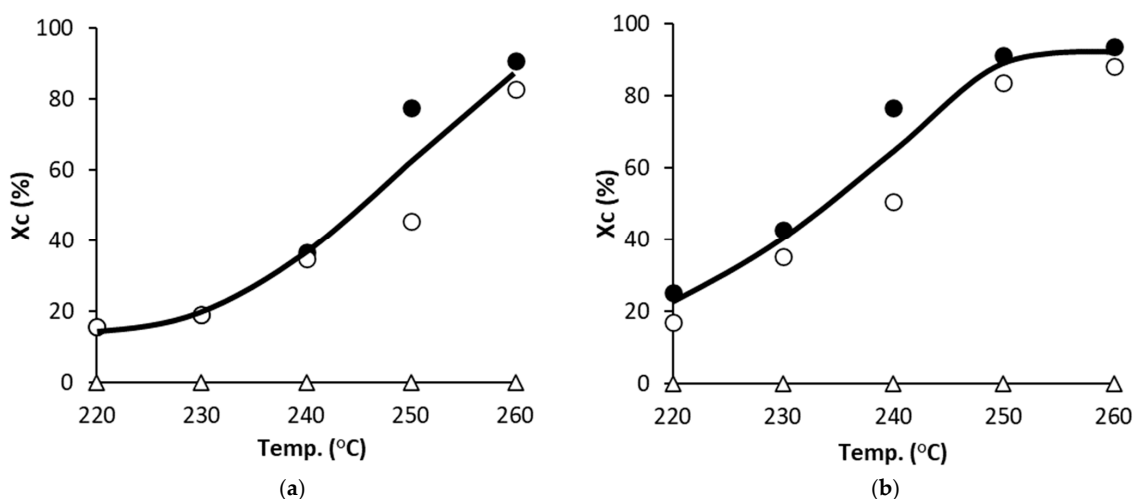

Figure 2. (**a**) Cellulose conversion (X_c) to products with reaction temperature. Two independent experiments under N_2, shown ((●), (○)), are for a starting cellulose concentration of 40 g.L^{-1}; (–) represents average X_c under N_2; (△) is the control experiment with no heat. (**b**) Cellulose conversion (X_c) to products with reaction temperature under CO_2; (●), (○) denote two independent experiments under CO_2; (–) represents average X_c under CO_2. Reaction pressure was from 60 to 90 bars. Cellulose conversion to products is the average of two experiments with variation between replicates within ±5%.

Substituting CO_2 for N_2 increased X_c, e.g., at 250 °C the conversion was 59.2 ± 12.8% and 73.3 ± 8.1% under N_2 and CO_2, respectively (mean ± SEM; 3 experiments). The use of CO_2 shifted down the products and TOC profiles by 10 °C and were comparable (Figure 3) with respect to the production of glucose, fructose or 5-HMF, which was approximately equimolar with glucose. The low fructose (Figure 3b) is consistent with it being the precursor of 5-HMF. Some decomposition of products occurred above 260 °C under N_2 and 250 °C under CO_2 (Figure 3).
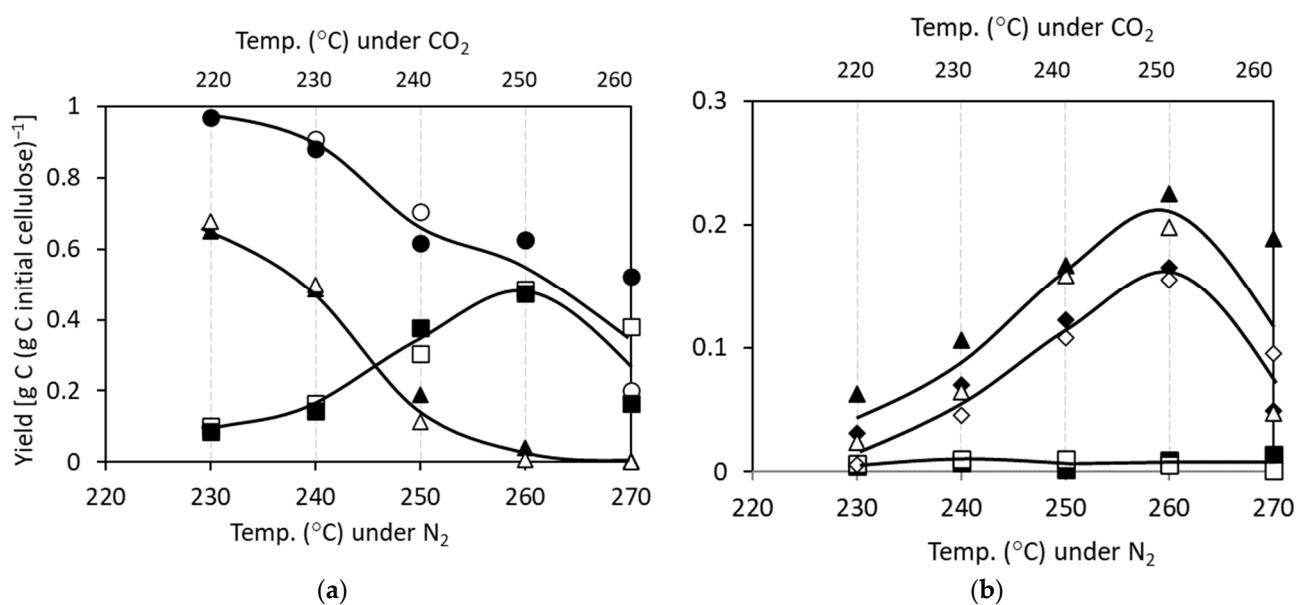

Figure 3. Total organic carbon (**a**) and product yield (**b**) in hydrolysates before AC under CO_2 (filled symbols) and N_2 (open symbols). a): (●,○), TOC total (hydrolysate + residue); (▲,△), TOC residue; (■,□), TOC hydrolysate. b): (▲,△), glucose; (■,□), fructose; (♦,◇), 5-HMF in hydrolysates. The TOC total does not include material lost in some samples due to precipitation, char in residue and gas composition, which was estimated to be less than 5%wt. Yield values are average of two experiments with variation between replicates within ±5%.

During hydrolysis, the pH of the hydrolysates fell from pH 6.3 to between 2.6 and 3.6. The solution chemistry of carbon dioxide in water and formation of carbonic acid (e.g., potentially giving some acid hydrolysis) are poorly understood under HCW reaction conditions; carbonic acid exists only transiently in solution [43]. The hydrolysate pH fell as low as pH 2.6 and would lead to different proportions of fully ionised/fully associated organic species over the conditions studied [44].

The glucose yield under CO_2 was, maximally, 0.225 g C/g C initial cellulose, (at 250 °C) while that under N_2 was 0.198 gC/gC initial cellulose at 260 °C, i.e., ~20% glucose yield in each case, which is ~half of the yield reported in similar experiments at 200 °C using starch [45], attributable to the recalcitrance of crystalline cellulose (see Introduction). The results shown in Figure 2 suggest that glucose contained in the hydrolysate would be suitable for fermentation provided that significant removal of toxic 5-HMF could be achieved.

2.1.2. Detoxification with AC

Glucose and organic acids were not removed significantly by AC treatment while, in contrast, more than 70% of 5-HMF co-product was removed from 37 mM (250 °C) and 35 mM (260 °C) 5-HMF produced under CO_2 and N_2, respectively (Figure 4). This is consistent with previous 5-HMF detoxification experiments with starch hydrolysates [45].
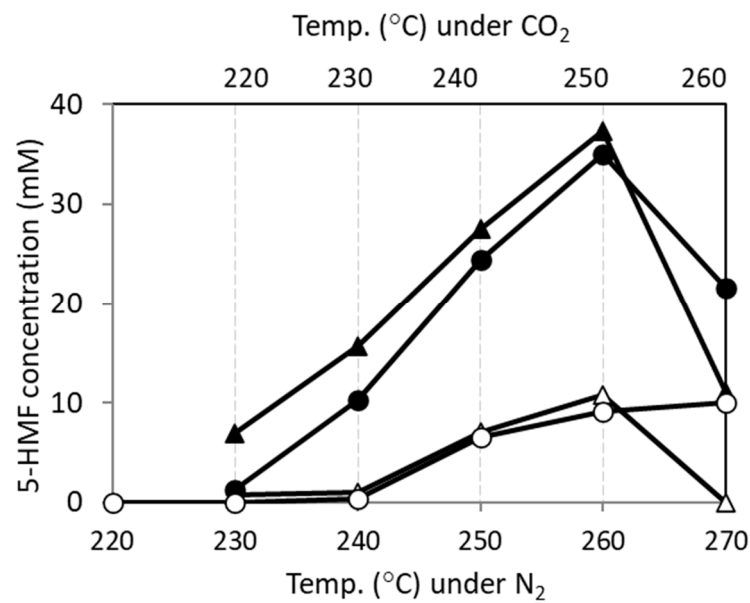
Figure 4. Concentrations (mM) of 5-HMF before (filled symbols) and after (open symbols) AC treatment for experiments prepared under CO_2 (▲,△) and N_2 (●,○) at different reaction temperatures. Results shown are average values of two experiments with variation within ±5%.

2.1.3. Growth of *E. coli* on Native and AC-Treated Hydrolysates, and Biohydrogen Production

AC-treated hydrolysates supported twice the growth of *E. coli* in comparison with the control with hydrolysates prepared at 240 °C and 250 °C (Figure 5a).

(**a**)

Figure 5. *Cont.*

(b)

Figure 5. (**a**) Growth of *E. coli* in hydrolysates prepared under CO_2 at different reaction temperatures (●) without and (○) with AC treatment. The dotted line re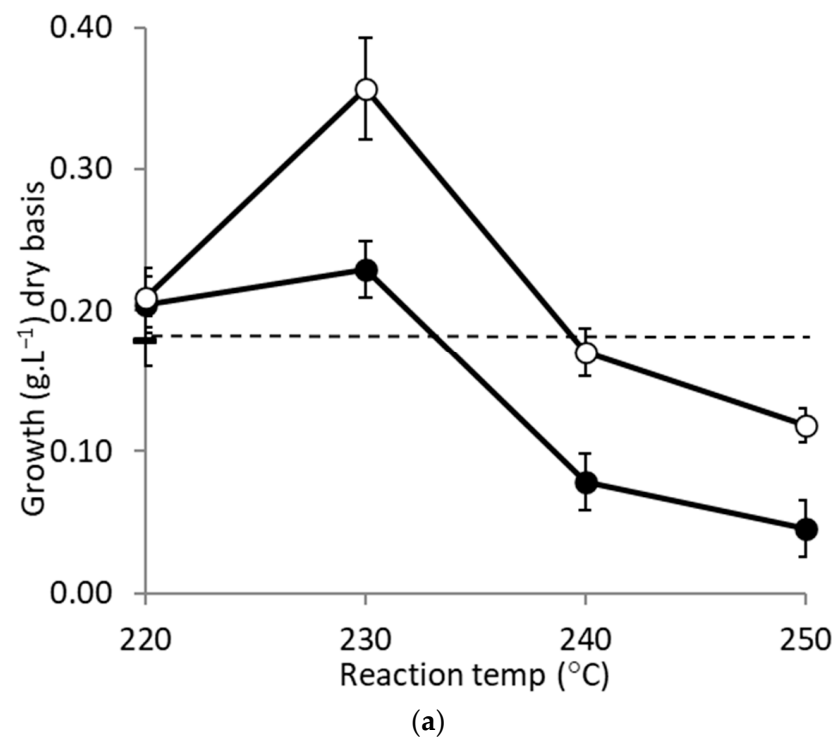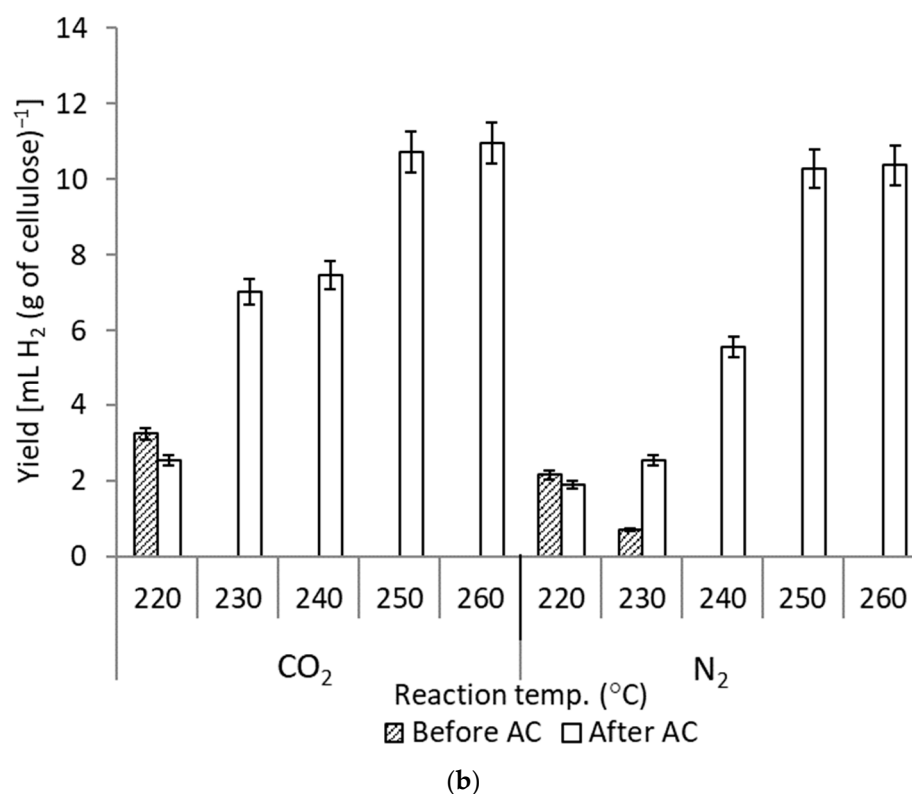presents the biomass yield from the glucose control (20 mM); (**b**) Hydrogen yields after fermentation of the hydrolysates produced at various temperatures. Under CO_2 no H_2 was produced before AC treatment from samples prepared at temperatures higher than 230 °C; under N_2 no H_2 was produced from samples prepared at above 240 °C before AC treatment. At 220 °C the concentration of 5-HMF in the hydrolysate is too low to cause total inhibition and H_2 is produced. As temperature increases, and the concentration of 5-HMF increases, the inhibitory effect is evident.

From the latter, untreated and treated samples gave 74% and 33% inhibition, respectively, indicating residual inhibitory degradation products (c.f. Figure 4). Growth was increased using AC by 1.5-fold using HCW cellulose hydrolysis under CO_2 at 230 °C (Figure 5a) but samples made at 240 °C showed no benefit on growth (Figure 4) even though much of the 5-HMF had been removed (Figure 4). Inhibition was attributed to the low pH; undissociated formic acid (pKa of 3.75) is highly toxic as it enters cells, dissociates in the neutral cytoplasm and H^+ kills the cells via low internal pH [46]. Against this, the hydrolysate was diluted 10-fold into the growth medium, which was buffered (pH 6.5 [45]). However, the extent of growth is relatively unimportant since bio-H_2 is made by resting cells, while biomass overgrowth may be undesirable as this requires disposal or up-valorisation (see later).

No H_2 was produced without AC treatment of cellulose hydrolysates made at temperatures above 230 °C and 220 °C with N_2 and CO_2, respectively (Figure 5b) attributed to inhibitory effects of co products of cellulose hydrolysis. In contrast, AC-treated hydrolysates supported H_2 production (following removal of co-product 5-HMF).

Hydrogen yields increased in parallel to the hydrolysis temperature in these bottle tests to, maximally, 10–11 mL H_2/g of cellulose from samples prepared at 250 and 260 °C in both cases (attributable to their higher glucose content), but with correspondingly ~31 to 37% lower yields as compared with those previously reported from starch hydrolysate made at 200 °C under CO_2 [45]. This H_2 yield is important, being key to the overall energy balance for process viability (see later).

2.2. Scope for Sustainable Biohydrogen Process for Bioenergy from Cellulose

2.2.1. Hydrogen Yield from the *E. coli* 'Dark' Fermentation

A simple calculation shows that biohydrogen production by *E. coli*, as shown here in the bottle tests, is not economically or energetically feasible for use with an example biomass such as *Miscanthus*: a production of 10–11 mL H_2/g of cellulose (above)(i.e., 100–110 kJ H_2/kg of cellulose) falls well short of the 184 kJ/kg required for biomass comminution alone, before factoring-in the lower yields obtained from real waste hydrolysate (above and Supplementary Materials Figure S2). The high energy density of liquid H_2 (if liquefaction is the chosen path for hydrogen utilisation) comes at the expense of significant compression and cooling costs [47]. Clearly the H_2 yield must be increased.

The simple 'bottle' fermentation tests in this study, yielding ~11 mL H_2 per g of cellulose (Figure 4), used cells fermenting, unmixed, for 24 h. A detailed study reported elsewhere using a well-mixed fermenter [48] showed that, via re-assimilation and re-consumption of part of the acetate produced from glucose, the hydrogen yield was increased by 50% between 24 and 48 h. By factoring this improvement into the current study, a hydrogen yield of ~16 mL per g of cellulose would be anticipated, but the projected energy yield (~160 kJ H_2/kg) still falls below the break-even point for the example comminution energy demand (see above).

Fermentative bio-H_2 production by *E. coli* is limited biochemically to 2 mol H_2 per mol of glucose (discussed in [41,49]). In addition to H_2 and CO_2, the fermentation products are ethanol and organic acids (OAs). An analysis of products was made for four strains of *E. coli* (R.L. Orozco and A.J. Stephen unpublished work) from the optimised 48-h fermentation [48], which takes into account the greater amount of hydrogen and a correspondingly lower acetate content due to its reassimilation and secondary fermentation into additional H_2 [48]. The concentration of ethanol product was 0.9 mol/mol sugar (comparable to the production of carbon in the OAs), which is too low for recovery by distillation. However, other studies have shown that a bio-Au catalyst bioresourced from jewellery waste by *E. coli* oxidises alcohol to the corresponding OA (see [34]) and a bio-Au 'trap' would approximately double the acetate content (from ethanol) of the spent fermentation medium for electrodialytic extraction and downstream secondary photo-fermentation (see below). If not removed, ethanol build-up in the dark fermentation inhibits the cells, requiring a 'fill and draw' as opposed to a continuous process.

The optimised dark fermentation biohydrogen process [48,49] was evaluated in the current context; note that the H_2 production shown in Table 1 is only ~18% of the maximum yield attainable from *E. coli* fermentation of hexose sugar (2 moles H_2/mole sugar), which was attributed to sub-optimal conditions in the small bottle tests. In contrast, ~80% conversion from glucose (a four-fold increase) was reported using a commercial well-mixed fermenter with automated pH regulation and agitation [41,49]. Hence, the working yield adjusted to optimal conditions was taken as 1.6 mol H_2/mol glucose for onward calculations.

2.2.2. Downstream Secondary Photo-Fermentation for a Coupled System

The ability of *Rhodobacter sphaeroides*, a purple-non-sulfur (PNS) bacterium, to generate bio-H_2 from the organic acid mix (OA mix) produced by *E. coli* [49] was evaluated by photo-fermentation, as described in Section 3. The synthetic OA mix concentration was adjusted to 20 mM as follows: acetate 6.7; lactate 3.8; succinate 5.2; butyrate 4.4. The hydrogen produced by this test was 1973 ± 252 mL H_2 (mean ± SD; 3 experiments).

A useful evaluation for a biohydrogen process is its hydrogen production potential (HPP) [50] defined as total hydrogen gas (mole) that can be produced per mole of OA. The HPP values are: acetate (2 carbons), 4; lactate (3 carbons), 6; butyrate (4 carbons) 10; succinate (4 carbons) 7 [41]. Hence, by taking the hydrogen yields obtained in this study in the above bottle photo-fermentation tests, the HPP of hydrolysates can be compared and the efficiency of the process calculated (HPP: potential mol hydrogen per mol of OA). This comparison is shown in Table 1 (below):

Table 1. H_2 generated in this study compared to HPP of the OA mix. STDEV with $n = 3$ (number of experiments).

Organic Acid (OA)	mmol in OA Mix	H_2 Produced by Mix (mol/mol OA Mix)	HPP (mol H_2/mol OA)	HPP by OA Mix (mol)
Acetate	6.7	0.081 ± 0.011	4	0.027
Lactate	3.8		6	0.023
Succinate	5.2		7	0.036
Butyrate	4.4		10	0.044
Total	20.1	0.081 ± 0.011		0.130

From these values, the yield of H_2 produced in this study was 4.05 mol H_2/mol OA. The conversion efficiency of the photo-fermentation test (EP) is calculated by Equation (1):

$$EP = \text{Hydrogen produced} \times \text{PPmix} \times 100. \tag{1}$$

From Equation (1), 62.3% of the total theoretical maximum H_2 production was achieved (under the conditions of the tests) giving good scope for process improvement through improvements in better controlled operation conditions (e.g., mixing, pH, culture density), light utilisation (which was calculated to be less than 2%: R.L. Orozco, unpublished work) and through better photobioreactor design and light 'upgrading'. The latter offers significant potential for photosynthetic process improvement. Promising results were achieved in a paradigm algal system by using quantum dots (made from wastes [51]) to up-convert unused wavelengths of sunlight into usable light, doubling the photo-synthetic yield [52]. However, unlike algae, PNS bacteria absorb light maximally in the near infrared (NIR) part of the spectrum. The development of NIR-emitting quantum dots is a relatively new technology and currently uneconomic in this application. The use of low energy light emitting diodes (LEDs) emitting at photo-synthetically active wavelengths is now common in horticulture. As with use of quantum dots, the application of an LED array more than doubled the photo-synthetic productivity using the microalga *Chlorella vulgaris* (R.L. Orozco, unpublished), but was then limited by the transfer of CO_2 to the cells; additional 2% CO_2 enhanced the photo-productivity by approximately 7-fold compared to air (R.L.Orozco, unpublished). Since PNS bacteria use fixed carbon (OAs), this limitation will not apply in the coupled bio-hydrogen fermentation. Biogas from *R. sphaeroides* is virtually all hydrogen under these conditions.

H_2 yields from photo-fermentation are significantly higher than from 'dark' fermentations. Hence, DF is more important as a supply of organic acids into the photo-fermentation than for its bio-H_2 production *per se*. Previous work (R.L. Orozco and A.J. Stephen, unpublished) showed that the H_2 yield in the photo-fermentation was independent of the organic acid proportions in the feed from the mixed-acid dark fermentation. Hence, any source of organic acids could be potentially used from a dual system or, indeed, in a stand-alone photo-fermentation (see later discussion), anticipating similar H_2 yields after photo-fermentation as those found in this study. This is important as the organic acid mix from other high producing *E. coli* strains (e.g., FTD67, FTD89, RL009, MC4100) can also be used as a source of OAs which can be efficiently transferred to the photo-fermentation system via electro-separation [39,41].

2.2.3. Scope for Development of a Dual Fermentation for Up-Conversion of Cellulose into a Positive Energy Balance

The hydrothermal treatment of cellulose (model compound) was used as the hydrolysis method to extract energy products. The actual energy yield from the dual fermentation tests using the extracted glucose can be estimated from their bio-H_2 yield. Dark fermentation in the bottle tests used in this study yielded 11 mL H_2/g of cellulose from samples prepared between 250 and 260 °C, with a total energy content equivalent to 0.031 kW·h/Kg cellulose. Photo-fermentation yielded 4.05 mol H_2/mol OA with a ten-fold

higher total energy content equivalent to 0.363 kW·h/Kg cellulose, clearly reinforcing the conclusion that dark fermentation is more important as a supply of organic acids into the photo-fermentation than for its bio-H$_2$ *per se*. The energy gained from DF alone still falls short of the 183 kJ/kg (0.051 KW·h/Kg) required for comminution of the example *Miscanthus* biomass (containing lignocellulosic compounds). However, the energy from photo-fermentation significantly surpasses comminution energy requirements. Process product yields and energy balance, taking into account additional energy demands, will be presented later.

2.3. Catalytic Upconversion of Cellulose Hydrolysate Side Stream into Liquid Fuel Precursor

2.3.1. Solvent Extraction of 5-Hydroxymethyl Furfural for One-Pot Catalysis

The liquid/liquid extraction method for 5-HMF extraction developed in previous studies [47,53] reported a MTHF extraction efficiency of 5-HMF from the aqueous phase from 59 to 63% resulting in 5-HMF concentrations in MTHF of c.a. 21 mM. The calculations of energy balance (later) will be based on this result.

2.3.2. Catalytic Up-Conversion of 5-HMF into DMF

In order to justify the use of post-fermentation *E. coli* to bio-manufacture and support a metallic catalyst, a comparison was made to the paradigm *D. desulfuricans* catalyst as the bio-Pd/Ru bimetallic. Although the latter organism makes highly effective metallic nanocatalysts (see Introduction), it is uneconomic to grow *D. desulfuricans* at scale 'for purpose', and is also challenging, due to its obligately anaerobic growth format and production of toxic H$_2$S. Bio-nanocatalysts made by the two organisms were characterised and compared by Gomez-Bolivar [54] and the upgrading of 5-HMF by both is compared in Table 2. The nominal catalyst composition was 5 wt% Pd/5 wt% Ru. Whereas all of the Pd(II) was removed onto the cells into Pd(0), the removal of Ru(III) was incomplete, giving actual catalyst compositions as shown in Table 2.

Table 2. One-pot catalytic upgrading of 5-HMF to 2,5-DMF in cellulose hydrolysate. Commercial catalyst ($_{comm}$); *Desulfovibrio desulfuricans* ($_{Dd}$) 5% Pd/5% Ru; *Escherichia coli* ($_{Ec}$) 5% Pd/5% Ru. ND: not determined. Errors between technical replicates and between experiments were within 10%. Bold: comparison between the two Gram-negative strains. This table contains average values of two experiments. Actual composition of bimetallic $_{Ec}$ was (5%Pd/4.7%Ru), 5%Ru$_{Ec}$ (2.6%Ru) [47].

Catalyst	Commercial 5-HMF		5-HMF from Cellulose Hydrolysate	
	Conversion (%)	Yield (%)	Conversion (%)	Yield (%)
No catalyst	15.5	33.4	ND	ND
5% Ru$_{comm}$	100	52.4	100	3.0
5% Pd$_{comm}$	100	6.4	ND	ND
Bimetallic$_{Dd}$	100	35.9	73.4	16.2
Bimetallic$_{Ec}$	100	54.4	77.6	24.1
5% Ru$_{E.c}$	100	11	72.6	19.1
5% Pd$_{Ec}$	100	51.1	ND	ND

The atomic weights of Pd and Ru are 106 and 101, respectively, hence, the nominal catalyst composition was ~equimolar but the available amount of each metal was not determined; both core-shell and alloyed nanostructures were reported as well as isolated monometallic 'islands' [54]. The *E. coli* bio-Pd/Ru catalyst was 34% and 33% better than the *D. desulfuricans* counterpart in the case of 5-HMF obtained commercially and that obtained from the hydrolysis of cellulose, respectively (Table 2). In each case, the DMF obtained from cellulose hydrolysate-5-HMF by the bio-catalysts was approximately half of that obtained from pure 5-HMF, which has adverse implications for bioprocess implementation. However, in contrast, the yield using a commercial Ru/C catalyst was 18-fold less in the hydrolysate than with pure 5-HMF (Table 2). This observation contrasts with an earlier study by Hu et al. [55] using a commercial

Ru/C catalyst where the use of pure 5-HMF or that made from bioresourced fructose, other sugars and cellulose had little effect on the yield of DMF from the extracted 5-HMF. Understanding the reason for the contrast between this report and the current work was outside the scope of this study, but it should be noted that, while the current work used hot compressed water only, Hu et al. [55] performed cellulose hydrolysis using a sulfonated carbonaceous catalyst in ionic liquid (1-butyl-3-methylimidazolium) chloride at 160 °C (15 min) followed by 5-HMF extraction. This introduces complexity and cost, whereas the present study (which is not yet optimised) pioneers a simple one-pot system for catalytic 5-HMF up-conversion in the cellulose hydrolysate directly following removal and up-conversion of the fermentable fraction.

Hu et al. [55] surveyed various catalysts, concluding that Ru/C outperformed others (Raney-Ni, Pd/C, Pt/C, Rh/C). An early study using *Bacillus benzeovorans* [38] showed the promise of bimetallic bio-Pd/Ru as compared to single metals. Table 2 shows that in this study the bio-Ru and bio-Pd/Ru behaved similarly against commercial 5-HMF but the bimetallic had better activity by 20% against the 5-HMF from cellulose hydrolysate (a similar improvement using the bimetallic to that observed by Omajali et al. [38]).

Despite the facility of a one-pot conversion from cellulose to DMF, it is clear that both the 5-HMF conversion and yield must be improved to give comparable activity to that of the more complex process of Hu et al. [55] commensurate with a favourable overall energy balance and cost (see later Discussion).

2.3.3. Calculation of Energy Balance Using Obtained Data

The cellulose hydrolysates yielded 1.25 mol glucose/kg cellulose which, after dark fermentation, delivered 0.45 mol H_2/Kg cellulose, which is ~8% of the hydrogen yielded by photo-fermentation (5.4 mol H_2/Kg cellulose), which comes from the OA mix generated by dark fermentation (1.33 mol OA mix/Kg cellulose). This highlights the importance of dark fermentation as source of OAs for photo-fermentation as a coupled fermentation process. The 5-HMF extracts (at 65% extraction efficiency) provided 5-HMF concentrations of 0.083 mol 5-HMF/Kg cellulose. The hydrolysate-extracted 5-HMF in MTHF (adjusted to the same concentration of 5-HMF in each test), catalytically upgraded to 2,5-DMF (Table 2) using the bio-Pd/Ru *E. coli* catalyst, yielded 0.159 mol DMF/Kg cellulose (Table 3).

Table 3. Cellulose hydrolysis, fermentation and hydrogenation yields of products. Glucose and 5-HMF yields from cellulose via hydrothermal hydrolysis are reported previously in this study. 5-HMF extraction in MTHF, efficiency and yields are from [48,53]. H_2-dark fermentation yields are reported in this study and from [48]. H_2-photo-fermentation H_2 yields are from [48,49,56] and R.L. Orozco (unpublished work). Catalytic hydrogenation of 5-HMF to 2,5 DMF yields are taken as per in [57]. Hydrothermal Hydrolysis (HTH); Extraction Efficiency (E.E.); Dark Fermentation (D.F.); Photo-fermentation (P.F.); Cellulose (C); Commercial (commer.). STDEV with n = 3 (number of experiments). Values without STDEV are average of two experiments.

Cellulose Hydrolysis and Fermentation Yields								Catalytic Hydrogenation of 5-HMF to 2,5 DMF Yields		
HTH Products		5-HMF Extraction in MTHF (1:1)		D.F. Yields		P.F. Yield		g DMF/g 5HMF		mol DMF/Kg C
(mol glucose/Kg C)	mol 5-HMF/Kg C	E.E. (%)	mol 5-HMF/Kg C	mol H_2/Kg C	mol OA mix/Kg C	mol H_2/mol OA mix	mol H_2/Kg C	5% Ru Commer.	5% Pd/5% Ru *E. coli*	5% Pd/5% Ru *E. coli*
1.25	0.127	65	0.083	0.45 ± 0.06	1.33 ± 0.17	4.05 ± 0.33	5.40 ± 0.43	0.023	0.183	0.159

In terms of the energy balance, Table 4 shows the projected energy output from biohydrogen (see above) and the amount of energy from 2,5-DMF obtained per kilo of starting cellulose, which together totals 0.537 kW·h/Kg cellulose. This amount is 15-fold smaller than the total energy input for the heat-consuming reactions (R1 + R2, Table 4), which amount to 8.18 kW·h/Kg cellulose.

Table 4. The energy balance of this work consisting of the energy input for the cellulose hydrolysis and hydrogenation reactions compared to the energy output obtained from the bio-H_2 yields of dark and photo-fermentation and 2,5 DMF obtained from the hydrogenation reaction. Dark Fermentation (D.F.); Photo-fermentation (P.F.). All calculations in this table were based on average values from experiments as described in this study.

Reactor 1 (R1: Hydrolysis of Cellulose to 5-HMF @ 250 °C)			Reactor 2 (R2: Hydrogenation of 5-HMF to 2,5 DMF @ 260 °C)				Energy Output (kW·h/Kg Cellulose)			
Cell. Load (Kg)	Water (kg)	Energy Input kW·h/Kg Cellulose	5-HMF in Reactor (g)	MTHF (Kg)	Energy Input kW·h/Kg Cellulose	Total Energy Input in R1 and R2	H_2 from D.F.	H_2 from P.F.	2,5 DMF from R2	Total Energy Output
0.008	0.125	4.56	0.250	0.0427	3.61	8.18	0.031	0.363	0.143	0.537

In any reaction that demands a significant amount of energy such as heat, an effective heat recovery system is critical to achieve energy efficiency. Assuming heat losses of 15% in a continuous reaction process, the heat supplied to make-up for these losses would need to be 1.23 kW·h/Kg cellulose. The total energy output would have to at least account for these losses to break even. In this case, it falls significantly short, rendering the integrated process energy inefficient as a means to realise energy from cellulose.

The maximum energy (calorific) output of the products on the basis of this study and other obtained data from related work is 0.537 kW·h/Kg cellulose (Table 4). Assuming no boosting via light 'upgrading' or advanced photobioreactor design, photofermentation provides a significant contribution, generating ~68% of the energy output. This is important as OAs (the PF feed) can be efficiently extracted from other abundant sources (see later discussion). The energy contribution from DMF is 27% of the energy output but only 5% comes from dark fermentation. Despite a good contribution of DMF to the total energy output, DMF contributes only 4% of the energy needed in the hydrogenation reaction, which is highly energy intensive, requiring 3.61 kW·h/Kg cellulose, i.e., 41% of the total energy input of the reactions, as seen in Table 4. This result has a significant negative impact on the economic viability of the overall process, considering also that the energy that would be needed for electro-separation and for the chemical extraction process were not included in the analysis. Hence, we conclude that, currently, in-process generation of DMF from the cellulose hydrolysate has limited potential without significant optimisation and, hence, the dual focus must now be on improving the catalysis component in tandem with other factors, working towards circularity.

2.4. Key Factors in Waste Up-Valorisation: Towards an Integrated Biorefinery Energy Process

The above discussion indicates that the energy products generated by the thermal-hydrolysis of cellulose (model compound used in this work) are currently incapable to provide, at the least, the energy needed for the overall process. In addition, in the valorisation of real lignocellulosic wastes, cellulose extraction from lignocellulosic biomass requires high 'parasitic' energy demand of upstream comminution, which is required to obtain a suitable particle size for cellulose extraction, which can then be efficiently achieved via delignification using environmentally friendly thermal subcritical water-ethanol-CO_2 mediated hydrolysis ($P_{initial}$ 55 bar; T_{final} 200 °C) [58,59]. Nontrivially, the energy consumption to mill *Miscanthus* (moisture content of 15%) to <4 mm was 184 kJ/kg of dry matter [60], which can be compared to a hydrogen energy content of only 10 kJ/litre at 1 atm and 15 °C and, hence, 18.4 L of H_2 would be 'consumed' per kilo of *Miscanthus* source material. Potentially mitigating against this total 'parasitic' energy demand (mechanical + thermal), the method [58] can drive biomass delignification without destroying the cellulose fibres, thereby generating two high value fractions: cellulose and lignin, the latter being an important source of aromatic compounds and chemicals [61]. In the case of cellulose, structural factors such as the reduction in crystallinity and increase in porosity as a result of the thermal treatment, make it potentially

more accessible to hydrolysis treatments, facilitating enzymatic-biocatalytic hydrolysis of the weakened cellulose structure, and/or reducing the generation of degradation products and increasing sugar yields from the thermal hydrolysis. These factors, while potentially further enhancing the cellulose extraction, and its hydrolysis process economics, were beyond the focus of this scoping study, which aimed to 'benchmark' the potential of a dual-biofuel production from cellulosic feedstock.

3. Materials and Methods

3.1. Chemicals, Microorganisms and Biomass Resources

D(+) glucose was from Fisher Scientific. Activated carbon (AC) was colorsorb 5 steam activated powder from JACOBI (micropore, 0.19 cm^3 g^{-1}; mesopore, 0.37 cm^3 g^{-1}; macropore. 1.68 cm^3 g^{-1}; total surface area: 900 m^2 g^{-1}). All other chemicals, cellulose microcrystalline powder, 5-HMF ($\geq$99%) and 2,5-DMF (99%) were from Sigma-Aldrich, as were commercial metal salts (Na_2PdCl_4 and $RuCl_3$) and 5 wt% Pd/C and 5 wt% Ru/C catalysts.

Desulfovibrio desulfuricans, a Gram-negative comparator to *Escherichia coli*, was grown as described previously [27]. *Escherichia coli* HD701, highly efficient in the dark fermentation of HCW hydrolysate, was obtained from laboratory stock. Bacterial cells, grown fermentatively and harvested as described in Orozco et al. 2012 [45], *Rhodobacter sphaeroides* (for downstream photo-fermentation of the organic acids produced by *E. coli*) was obtained, grown and harvested as described previously by Redwood et al. 2012 [39]. For adaptation, the same OA mix from the *E. coli* HD701 mixed acid fermentation of glucose was included in the synthetic OA media for initial growth and later for H_2 production tests. Carbon sources for the growth media were supplied to form a 40 mM solution as follows: acetate 13.3 mM; lactate 7.5 mM; succinate 10.4 mM and butyrate 8.8 mM. Cells were washed twice in 100 mL of phosphate buffered saline (PBS: 1.43 g Na_2HPO_4, 0.2 g KH_2PO_4, 0.8 g NaCl, 0.2 g KCl /L, pH 7.0) before storing the cell pellet at 4 °C.

3.2. Hot Compressed Water (HCW) Hydrolysis of Cellulose

HCW hydrolysis used a 250 cm^3 reactor (Parr series 4570/80 HP/HT; Parr Instruments Company, Moline, IL, USA equipped with a heat/agitation controller (model 4836) and a cooling system (Grant LTD6/20).

Cellulose (5 g) was suspended in de-ionised water (DW) to a final reactant volume of 125 cm^3 (40 g/L), leaving a headspace of 120 cm^3. The reactor was sealed and purged with N_2 or CO_2 gases for 3 min with agitation (850 rpm) before pressurising to 30 bar with N_2 (or CO_2) and heating to set-point temperature (temperature range from 220–260 °C). Reaction conditions were held for 15 min before rapid cooling to 100 °C; the reactor was removed from the heating vessel and quenched in an ice-water bath. The reactor was depressurised and the hydrolysate was separated from the solid residue by vacuum filtration through two layers of filter paper (Fisherbrand QL100). The residue was washed with distilled water, dried at 60 °C and weighed. The hydrolysates were analysed for total organic carbon (TOC) using a TOC analyser (Model TOC 5050A, Shimadzu Co., Tokyo, Japan). Organic acids were analysed by anion HPLC using a Dionex 600-series system as described previously [62]. Sugars, 5-HMF and furfural were analysed by HPLC (Agilent 1100 series) equipped with on-line degasser, quaternary pump, auto-sampler and RI detector (1200 series) as detailed in [45]; gases were not collected or analysed. For the estimation of residual polyglucose, the residue was acid-hydrolysed [53], and the glucose product was analysed by the dinitrosalicylic assay method [56]. Hydrolysates and samples were stored at −20 °C. When, occasionally, precipitate appeared in the samples after defrosting they were filtered to remove the solid residue which was not analysed. Reaction conversions (Xp) were calculated according to: [(Initial sample concentration (ISC)-residue after the reaction)/ISC] × 100; ISC and residues are expressed in g (dry basis)/L. Several preparations at 260 °C were pooled to give samples for extraction and, as appropriate, onward catalytic upgrading.

3.3. Detoxification of Cellulose Hydrolysates Using Activated Carbon, Fermentative Biohydrogen Production by E. coli and Downstream Photo-Fermentation by Rhodobacter spp.

Cooled cellulose hydrolysates were treated with 5% (w/v) activated carbon as described by Orozco et al., 2012 [45]. The pH, not adjusted, was measured before and after hydrolysis. Treated hydrolysates and untreated controls were vacuum-filtered (Fisherbrand QL100 filter paper). Samples were kept at -20 °C until use.

The *E. coli* strain HD701 was grown, harvested and used for fermentation tests on untreated and treated cellulose hydrolysate as described previously for starch [45]. Routine measurement of H_2 concentration (averages of 3 tests each) used a combustible gas meter (Gasurveyor2, GMI) and was estimated as described in Orozco et al., 2012 [40].

For H_2 production tests, washed cells of *Rhodobacter* spp. (from 3.1) were resuspended in 20 mL of PBS to produce a concentrate containing >4 g dry wt./L (calculated from OD_{660} via a previously determined conversion) and dispensed at a final concentration of 1 g dry wt./L in 5 mL aliquots of mixed organic acid media containing total 20 mM as follows: acetate 6.7; lactate 3.8; succinate 5.2; butyrate 4.4 into 15 mL glass reactors as described by Redwood [41]. Controls used cells in media omitting carbon sources. Reactors were sealed using butyl rubber stoppers with aluminium crimp seals and purged with Ar (15 min) before incubation (30 °C, static, 75 W/m^2 tungsten lamp, 72 h). Hydrogen was measured regularly by measuring the gas accumulated in the headspace of the bottles and the headspace pressure was determined as described by Ishaq [63].

3.4. Liquid–Liquid Separation of Soluble Fermentable Fraction from Degradation Products

Further to fermentability 'scoping' tests using native and AC-detoxified hydrolysate, a method for liquid–liquid extraction of 5-HMF was developed from the partition coefficients as given by Blumenthal et al. [25]. The mass transfer of 5-HMF from the aqueous to the organic phase was optimal at 60 °C (routinely adopted), 5-HMF added in a concentration range from 1–5 wt% in the aqueous feed, impacted minimally on the partition coefficients (not shown) into organic extraction solvent 2-methyl tetrahydrofuran (MTHF). For extraction, the cellulose hydrolysates were mixed in equal volumetric proportions with 2-MTHF in an Erlenmeyer flask as described by Mikheenko et al. [27]. The organic phase (top) contained 5-HMF and other components (noted where appropriate) and the aqueous phase (bottom) contained fermentable sugars and OAs. Extracts were stored at -20 °C until use, with samples analysed by GC as described in [27]. Solvent extraction efficiency was calculated according to extraction efficiency (%) = moles of 5-HMF in organic layer/moles of 5-HMF in the aqueous layer.

3.5. Metallic Catalysts Made Using D. desulfuricans and Post-Fermentation E. coli

The bimetallic Bio-Pd-Ru catalyst (nominally 5%Pd/5%Ru, or as shown) on dry *D. desulfuricans* or *E. coli* was made as described previously [27,54,57]. The 2 mM Pd (II) solution was reduced to Pd(0) on the cells under high purity H_2 supplied by BOC UK, (30 min; complete removal (by assay) of residual soluble metal) to give 5 wt% bio-Pd(0). The bio-Pd(0) was washed twice (distilled water, DW), and added as a concentrated suspension into 1 mM Ru (III) solution (final concentration; volume was adjusted to give the required final metal loading on cells) to give a final loading of (nominally) 5 wt% Pd/5 wt% Ru. The actual composition of the catalyst was determined by assay of the residual solution [56,57] following (sequential) metal uptake (Pd then Ru) and was 5 wt% Pd with the Ru content as shown. The bio-Pd/Ru mixture was left to stand then saturated with H_2 (as above; 180 rpm, 30 °C; 96 h). The presumptive bio-nanoparticles were washed three times (DW) and once with acetone (9000× g, 15 min, 4 °C), air-dried and ground manually.

3.6. Catalytic Upgrading of 5-HMF to 2,5-DMF

The reactions (catalytic transfer hydrogenations) were carried out in a 100 mL stainless steel Parr reactor series 4590 directly (260 °C) in the MTHF extract using (nominally) 5%Pd/5%Ru on dry *E. coli* as described previously [27]. The tests used (i) commercially

obtained 5-HMF or (ii) 5-HMF obtained from cellulose hydrolysis following extraction into solvent as above. In (i) the reactor was charged with 250 mg of commercial 5-HMF (80 mM) in 25 mL of MTHF; the other tests used appropriate volumes of 5-HMF in MTHF extracted from the cellulose hydrolysates (to the same concentration of 5-HMF).

3.7. Analysis of Residual 5-HMF, 2,5 DMF and Other Products in the Catalytic Conversion Reaction

Samples were analysed using a GC-FID for quantification and a GCMS-QP2010s for compound identification. All GC-FID analysis was performed on a Shimadzu GC2014 equipped with a Shimadzu AOC-20i autosampler as described previously [27,54,57].

5-HMF conversions and 2,5 DMF yields were calculated as follows:

$$\text{HMF conversion (\%)} = 1 - (\text{moles of HMF in products/starting moles HMF}) \times 100;$$

$$\text{DMF yield (\%)} = (\text{moles of DMF in products/starting moles HMF}) \times 100;$$

$$\text{DMF selectivity (\%)} = [1 - (\text{moles of DMF in products/(starting moles 5-HMF-final moles 5-HMF})] \times 100.$$

4. Conclusions

The hydrothermal liquefaction of cellulose (model compound) yielded 4.5 mol of H_2/Kg of cellulose and 0.159 mol of 2,5 DMF/Kg of cellulose; this is equivalent to a potential energy output of 0.537 KW·h/Kg cellulose. The energy input for the hydrolysis and hydrogenation reactions amounts to 8.18 KW·h/Kg cellulose, which exceeds the energy output by 15-fold. The negative energy balance leads us to conclude that the overall process is energetically unfeasible; the energy balance is rarely considered or discussed in the (large) biotechnology literature. This study stresses the importance of energy projections in advance of a programme of research and development.

When using real lignocellulosic wastes, the energy needed for the comminution (0.051 KW·h/Kg material) (see earlier) and extraction of cellulose from the lignin will significantly further worsen the energy balance compared to that obtained with cellulose, thereby reinforcing the conclusion that the process utilised in this work using real lignocellulosic waste as a source of cellulose will be energetically and economically unviable. This overall conclusion would, without significant advances in the catalytic upgrading of the 5-HMF (and other side stream products—see Discussion and Supplementary Materials), significantly impact upon a key future role for biorefinery as a candidate for energy from lignocellulosic wastes, steering the 'landscape' in favour of other approaches such as e.g., supercritical water liquefaction or gasification. These do not require an extraction step but are also energy-demanding; here, a similar analysis awaits the outcome of ongoing studies, implementing the recycling of low-grade heat.

Particular attention should be given to the photo-fermentation of organic acids. In this work, OAs were able to generate 4.05 mol of H_2/mol of OA_{mix}, thereby contributing to generate c.a. 67% of the total energy output. These results demonstrated that the organic acids (OAs) are a potentially significant source of bio-H_2 and energy.

OAs are typically present in municipal wastewater treatment plants (e.g., 300,000 m^3/day; OA content 4 g/L) [55]. The realisation of energy production potential using the photo-fermentation of such waste OAs has been shown; 1000 MW p.a was achievable using biogas from 'traditional' wastewater treatment, which was doubled by OA photo-fermentation into H_2 by *Rhodobacter sphaeroides*, bypassing a dedicated dark fermentation [49]. In addition to wastewater, the acetogenesis (first) phase of anaerobic digestion (AD) offers scope for electrodialytic intervention with a photo-fermentation loop of extracted OAs to value-add to the final biogas, e.g., via production of 'hythane'. This mixture of hydrogen and AD-methane is compatible with current gas grids and yields more energy than methane alone [64]. As such, retrofitting a photo-fermentation 'loop' into existing waste treatment processes may be a shorter-term interim advance, pending more productive biorefinery development.

With respect to solid waste, such as we consider here, the Cambi process is an example of a successful application of thermal hydrolysis treatment under milder conditions together with a very effective heat recovery system, bringing a positive energy balance. This process hydrolyses and disintegrates sludge from wastewater treatment plants (up to 18% total solids, 160 °C, 6–10 bars, 20–30 min retention time) generating a low viscosity sterilised liquid that is easily digested in an anaerobic digestion reactor (and, hence, would be potentially useful for adding a photo-fermentation loop; see above). Operating conditions were sustained during 15 days of hydraulic retention time under mesophilic conditions (37 °C); pH 7; digestor load at 100 t dry solids/day. As a result, biogas and electricity production increased by 20% at least, with 40% decrease in final sludge volume as compared to conventional digestion. With optimal operation of the thermal hydrolysis plant, the net energy ratio of the additional biogas is approximately 3 times in relation to the parasitic energy needed in a continuous process [65,66].

Supplementary Materials: The following supporting information can be downloaded at: https://www.mdpi.com/article/10.3390/catal12060577/s1, Figure S1: Increase in sugar content of hydrolysate (%) by the application of ohmic heating (A), Hydrogen production potential of the hydrolysate (B), HPLC chromatogram of OH treated fruit wastes show higher content of organic acids (substrates for downstream photobiological hydrogen production) (C). In addition, a new peak (unidentified) is apparent following ohmic treatment of the waste (open arrow) [67]; Figure S2: Yields of products in brewery grain hydrolysates before AC at different reaction temperatures; Figure S3: Yields of products of wheat straw hydrolysate before AC at 220 and 240 °C. References [67–80] are cited in the Supplementary Materials.

Author Contributions: R.L.O. performed the cellulose hydrolysis (with G.A.L.), developed the liquid–liquid extraction of 5-HMF from hydrolysate, and performed *E. coli* fermentations of the hydrolysate. R.L.O. authored the first draft and carried out the energy balances. He also oversaw the *R. sphaeroides* biohydrogen tests, carried out with A.J.S., I.P.M. and M.L.M., oversaw the catalysis studies, carried out by J.G.-B., L.E.M., integrated the work and authored the draft to include the catalysis and up-valorisation, with contributions from all authors into the final manuscript, first-authored by J.G.-B. and R.L.O. All authors have read and agreed to the published version of the manuscript.

Data Availability Statement: Not applicable.

Conflicts of Interest: The authors declare no conflict of interest.

References

1. Tokarska, K.B.; Gillet, N.P.; Weaver, A.J.; Arora, Y.K.; Eby, M. The climate response to five trillion tonnes of carbon. *Nat. Clim. Chang. Lett.* **2016**, *6*, 851–855. [CrossRef]
2. Dębowski, M.; Dudek, M.; Zieliński, M.; Nowicka, A.; Kazimierowicz, J. Microalgal hydrogen production in relation to other biomass-based technologies—A Review. *Energies* **2021**, *14*, 6025. [CrossRef]
3. Park, J.-H.; Chandrasekhar, K.; Jeon, B.-H.; Jang, M.; Liu, Y.; Kim, S.-H. State-of-the-art technologies for continuous high-rate biohydrogen production. *Bioresour. Technol.* **2021**, *320*, 124304. [CrossRef] [PubMed]
4. Anonymous. Hydrogen Generation Market by Generation & Delivery Mode, Technology, Application & Region—Global Forecast to 2021. Available online: http://www.marketsandmarkets.com/Market-Reports/hydrogen-generation-market-494.html (accessed on 21 June 2016).

5.   Macaskie, L.E.; Baxter-Plant, V.S.; Creamer, N.J.; Humphries, A.C.; Penfold, D.W.; Yong, P. Applications of bacterial hydrogenases in waste decontamination, manufacture of novel bionanomaterials in sustainable energy. *Biochem. Soc. Trans.* **2005**, *33*, 71–79. [CrossRef]

6.   Sasaki, M.; Ohsawa, K. Hydrolysis of lignocellulosic biomass in hot-compressed water with supercritical carbon dioxide. *ACS Omega* **2021**, *6*, 14252–14259. [CrossRef]

7.   Dogaris, I.; Karapati, S.; Mamma, D.; Kalogeris, E.; Kekos, D. hydrothermal processing and enzymatic hydrolysis of sorghum bagasse for fermentable carbohydrates production. *Biores. Technol.* **2009**, *100*, 6543–6549. [CrossRef]

8.   Dadwal, A.; Sharma, S.; Satyanarayana, T. Thermostable cellulose saccharifying microbial enzymes: Characteristics, recent advances and biotechnological applications. *Int. J. Biol. Macromol.* **2021**, *188*, 226–244. [CrossRef]

9.   Horn, S.J.; Vaaje-Kolstad, G.; Westering, B.; Eijsink, V.G.H. Novel enzymes for the degradation of cellulose. *Biotechnol. Biofuels* **2012**, *5*, 45–60. [CrossRef]

10. Duff, S.J.B.; Murray, W.D. Bioconversion of forest products industry waste cellulosics to fuel ethanol: A review. *Biores. Technol.* **1996**, *55*, 1–33. [CrossRef]

11. Mok, W.S.; Antal, M.J.; Varhegyi, G. Productive and parasitic pathways in dilute acid-catalyzed hydrolysis of cellulose. *Ind. Eng. Chem. Res.* **2002**, *31*, 94–100. [CrossRef]

12. Liao, Y.; Beeck, B.; Thielemans, K.; Ennaert, T.; Snelders, J.; Dusselier, M.; Courtin, C.; Sels, B. The role of pretreatment in the catalytic valorization of cellulose. *Mol. Catal.* **2020**, *487*, 110883. [CrossRef]

13. Kamio, E.; Takahashi, S.; Noda, H.; Fukuhara, C.; Okamura, T. Effect of heating rate on liquefaction of cellulose by hot compressed water. *Chem. Eng. J.* **2008**, *137*, 328–338. [CrossRef]

14. Minowa, T.; Zhen, F.; Ogi, T.; Varhegyi, G. Liquefaction of cellulose in hot compressed water using sodium carbonate: Products distribution at different reaction temperatures. *J. Chem. Eng.* **1997**, *30*, 186–190. [CrossRef]

15. Minowa, T.; Zhen, F.; Ogi, T. Cellulose decomposition in hot-compressed water with alkali or nickel catalyst. *J. Supercrit. Fluids* **1998**, *13*, 253–259. [CrossRef]

16. Miyazawa, T.; Funazukuri, T. Polysaccharide hydrolysis accelerated by adding carbon dioxide under hydrothermal conditions. *Biotechnol. Prog.* **2005**, *21*, 1782–1785. [CrossRef]

17. Irmak, S.; Kurtuluş, M.; Hasanoğlu, A.; Erbatur, O. Gasification efficiencies of cellulose, hemicellulose and lignin fractions of biomass in aqueous media by using Pt on activated carbon catalyst. *Biomass Bioenergy* **2013**, *30*, 102–108. [CrossRef]

18. Pipitone, G.; Zoppi, G.; Frattini, A.; Bocchini, S.; Pirone, R.; Bensaid, S. Aqueous phase reforming of sugar-based biorefinery streams: From the simplicity of model compounds to the complexity of real feeds. *Catal. Today* **2020**, *345*, 267–279. [CrossRef]

19. Meng, X.; Ragauskas, J. Recent advances in understanding the role of cellulose accessibility in enzymatic hydrolysis of lignocellulosic substrates. *Curr. Opin. Biotechnol.* **2014**, *27*, 150–158. [CrossRef]

20. Mills, T.Y.; Sandoval, N.R.; Gill, R.T. Cellulosic hydrolysate toxicity and tolerance mechanisms in *Escherichia coli*. *Biotechnol. Biofuel.* **2009**, *2*, 26. [CrossRef]

21. Ezeji, T.; Qureshi, N.; Blaschek, H.P. Butanol production from agricultural residues: Impact of degradation products on *Clostridium beijerinckii* growth and butanol fermentation. *Biotechnol. Bioeng.* **2007**, *97*, 1460–1469. [CrossRef]

22. Hodge, D.B.; Andersson, C.; Berglund, K.A.; Rova, U. Detoxification requirements for bioconversion of softwood dilute acid hydrolyzates to succinic acid. *Enzym. Microb. Technol.* **2009**, *44*, 309–316. [CrossRef]

23. Palmqvist, E.; Hahn-Hägerdal, B. Fermentation of lignocellulosic hydrolysates. I: Inhibition and detoxification. *Bioresour. Technol.* **2000**, *74*, 17–24. [CrossRef]

24. Carter, B.; Gilcrease, P.C.; Menkhaus, T.J. Removal and recovery of furfural, 5 hydroxymethyl-furfural, and acetic acid from aqueous solutions using a soluble polyelectrolyte. *Biotechnol. Bioeng.* **2011**, *108*, 2046–2052. [CrossRef] [PubMed]

25. Blumenthal, L.C.; Jens, C.M.; Ulbrich, J.; Schwering, F.; Langrehr, T.; Turek, K.; Kunz, U.; Leonhard, K.; Palkovits, R. Systematic identification of solvents optimal for the extraction of 5-hydroxymethylfurfural from aqueous reactive solutions. *ACS Sustain. Chem. Eng.* **2016**, *4*, 228–235. [CrossRef]

26. Aycock, D.F. Solvent applications of 2-methyltetrahydrofuran in organometallic and biphasic reactions. *Org. Process Res. Dev.* **2007**, *11*, 156–159. [CrossRef]

27. Mikheenko, I.; Gomez-Bolivar, J.; Merroun, M.L.; Macaskie, L.E.; Sharma, S.; Walker, M.; Hand, R.A.; Grail, B.; Johnson, D.B.; Orozco, R.L. Upconversion of cellulosic waste into a potential 'drop in fuel' via novel catalyst generated using *Desulfovibrio desulfuricans* and a consortium of acidophilic sulfidogens. *Front. Microbiol.* **2019**, *10*, 970. [CrossRef]

28. Zhorg, S.; Daniel, R.; Xu, H.; Zhang, J.; Turner, D.; Wyszynski, M.L.; Richards, P. Combustion and emission of 2,5-dimethylfuran in a direct-injection spark-ignition engine. *Energy Fuels* **2010**, *24*, 2891–2899.

29. Davis, S.E.; Houk, L.R.; Tamargo, E.E.; Datye, A.K.; Davis, R.J. Oxidation of 5-hydroxymethylfurfural over supported Pt, Pd and Au catalysts. *Catal. Today* **2011**, *160*, 55–60. [CrossRef]

30. Tong, X.; Ma, Y.; Li, Y. Biomass into chemicals: Conversion of sugars to furan derivatives by catalytic processes. *Appl. Catal. A Gen.* **2011**, *385*, 1–13. [CrossRef]

31. Omajali, J.B. Novel Bionanocatalysts for Green Chemistry Applications. Ph.D. Thesis, University of Birmingham, Birmingham, UK, 2015.

32. Zhu, J.; Wood, J.; Deplanche, K.; Mikheenko, I.P.; Macaskie, L.E. Selective hydrogenation using palladium bioinorganic catalyst. *Appl. Catal. B Environ.* **2016**, *199*, 108–122. [CrossRef]

33. Orozco, R.L.; Redwood, M.D.; Yong, P.; Caldelari, I.; Sargent, F.; Macaskie, L.E. Towards an integrated system for bio-energy: Hydrogen production by Escherichia coli and use of palladium-coated waste cells for electricity generation in a fuel cell. *Biotechnol. Lett.* **2010**, *32*, 1837–1845. [CrossRef] [PubMed]

34. Murray, A.J.; Mikheenko, I.P.; Deplanche, K.; Omajali, J.B.; Gomez-Bolivar, J.; Merroun, M.L.; Macaskie, L.E. Chapter 9: Biorefinjng of metallic wastes into new nanomaterials for green chemistry, environment and energy. In *Resource Recovery from Wastes: Towards a Circular Economy*; Macaskie, L.E., Sapsford, D.J., Mays, W.M., Eds.; Royal Society of Chemistry: London, UK, 2020; pp. 215–240. ISBN 978-1-78801-381-9.

35. Archer, S.A.; Murray, A.J.; Omajali, J.B.O.; Paterson-Beedle, M.; Sharma, B.K.; Wood, J.; Macaskie, L.E. Chapter 13: Metallic wastes into new processes catalysts: Life cycle and environmental benefits within integrated analyses using selected case histories. In *Resource Recovery from Wastes: Towards a Circular Economy*; Macaskie, L.E., Sapsford, D.J., Mays, W.M., Eds.; Royal Society of Chemistry: London, UK, 2020; pp. 315–342. ISBN 978-1-78801-381-9.

36. Hallenbeck, P.C. *Microbial Technologies in Advanced Biofuels Production*; Springer: Berlin/Heidelberg, Germany, 2012; pp. 3–269.

37. Yong, P.; Mikheenko, I.P.; Deplanche, K.; Redwood, M.D.; Macaskie, L.E. Biorefining of precious metals from wastes: An answer to manufacturing of cheap catalysts for fuel cells and power generation via an integrated biorefinery? *Biotechnol. Lett.* **2010**, *35*, 1821–1828. [CrossRef] [PubMed]

38. Omajali, J.B.; Gomez-Bolivar, J.; Mikheenko, I.P.; Sharma, S.; Kayode, B.; Al-Duri, B.; Banerjee, D.; Walker, M.; Merroun, M.L.; Macaskie, L.E. Novel catalytically active Pd/Ru bimetallic nanoparticles synthesised by *Bacillus benzeovorans*. *Sci. Rep.* **2019**, *9*, 4175. [CrossRef] [PubMed]

39. Redwood, M.D.; Orozco, R.L.; Majewski, A.J.; Macaskie, L.E. An integrated biohydrogen refinery: Synergy of photofermentation, extractive fermentation and hydrothermal hydrolysis for food waste. *Biores. Technol.* **2012**, *119*, 384–392. [CrossRef] [PubMed]

40. Orozco, R.L.; Mikheenko, I.P.; Omajali, J.B.; Macaskie, L.E. Chapter 3: Biohydrogen production from agricultural and food wastes and potential for side stream valorisation from waste hydrolysates. In *Resource Recovery from Wastes: Towards a Circular Economy*; Macaskie, L.E., Sapsford, D.J., Mays, W.M., Eds.; Royal Society of Chemistry: London, UK, 2020; pp. 57–86. ISBN 978-1-78801-381-9.

41. Redwood, M.D. Bio-Hydrogen Production and Biomass-Supported Palladium Catalyst for Energy Production and Waste Minimization. Ph.D. Thesis, University of Birmingham, Birmingham, UK, 2007.

42. Orozco, R.L.; Redwood, M.D.; Leeke, G.A.; Bahari, A.; Santos, R.C.D.; Macaskie, L.E. Hydrothermal hydrolysis of starch with CO_2 and detoxification of the hydrolysates with activated carbon for bio-hydrogen fermentation. *Int. J. Hydrog. Energy* **2012**, *37*, 6545–6553. [CrossRef]

43. Redwood, M.D.; Macaskie, L.E. A two-stage, two-organism process for biohydrogen from glucose. *Int. J. Hydrog. Energy* **2006**, *31*, 1514–1521. [CrossRef]

44. Saeman, J.F.; Bubl, J.L.; Harris, E.E. Quantitative saccharification of wood and cellulose. *Ind. Eng. Chem. Anal. Ed.* **2002**, *17*, 35–37. [CrossRef]

45. Chaplin, M.F. Monosaccharides. In *Carbohydrate Analysis: A Practical Approach*; Chaplin, M.F., Kennedy, J.F., Eds.; IRL Press; Oxford University Press: Oxford, UK, 1986; p. 3.

46. Ishaq, F. Trace Metal Supplementation in Wastewater Sludge Digesters. Ph.D. Thesis, University of Birmingham, Birmingham, UK, 2012.

47. Gomez-Bolivar, J.; Mikheenko, I.P.; Orozco, R.L.; Sharma, S.; Banerjee, D.; Walker, M.; Hand, R.A.; Merroun, M.L.; Macaskie, L.E. Synthesis of Pd/Ru bimetallic nanoparticles by *Escherichia coli* and potential as a catalyst for upgrading 5-hydroxymethyl furfural into liquid fuel precursors. *Front. Microbiol.* **2019**, *10*, 1276. [CrossRef]

48. Gomez-Bolivar, J. Synthesis of Palladium and Ruthenium Nanoparticles from Metal Solutions Using Bacteria with Application as Nanocatalyst. Ph.D. Thesis, University of Granada, Granada, Spain, 2019.

49. Sakaki, T.; Shibata, M.; Miki, T.; Hirosue, H.; Hayashi, N. Decomposition of cellulose in near-critical water and fermentability of the products. *Energy Fuels* **1996**, *10*, 684–688. [CrossRef]

50. Lam, R.K.; England, A.H.; Sheardy, A.T.; Shih, O.; Smith, J.W.; Rizzuto, A.M. The hydration structure of aqueous carbonic acid from X-ray absorption spectroscopy. *Chem. Phys. Lett.* **2014**, *614*, 282–286. [CrossRef]

51. Toews, K.L.; Shroll, R.M.; Wai, C.M. pH-Defining equilibrium between water and supercritical CO_2. influence on SFE of organics and metal chelates. *Anal. Chem.* **1995**, *67*, 4040–4043. [CrossRef]

52. Hallberg, K.; Johnson, D.B. Biodiversity of acidophilic prokaryotes. *Adv. Appl. Microbiol.* **2001**, *49*, 37–84. [PubMed]

53. Stolzenburg, K.; Mubbala, R. *Integrated Design for Demonstration of Efficient Liquefaction of Hydrogen (IDEALHY) Hydrogen Liquefaction Report*; EU Grant No 2781772013; IDEALHY: Maastricht, The Netherlands, 2013.

54. Orozco, R.L. Hydrogen Production from Biomass by Integrating Thermo-Chemical and Biological Processes. Ph.D. Thesis, University of Birmingham, Birmingham, UK, 2011.

55. Stephen, A.J.; Archer, S.A.; Orozco, R.L.; Macaskie, L.E. Advances and bottlenecks in microbial hydro-gen production. *Microb. Biotechnol.* **2017**, *10*, 1120–1127. [CrossRef] [PubMed]

56. Eroğlu, E.; Gündüz, U.; Yücel, M.; Türker, L.; Eroğlu, I. Photobiological hydrogen production by using olive mill wastewater as a sole substrate source. *Int. J. Hydrog. Energy* **2004**, *29*, 163–171. [CrossRef]

57. Murray, A.J.; Roussel, J.; Rolley, J.; Woodhall, F.; Mikheenko, I.P.; Johnson, D.B.; Gomez-Bolivar, J.; Merroun, M.L.; Macaskie, L.E. Biosynthesis of zinc sulfide quantum dots using waste off-gas from a metal bioremediation process. *RSC Adv.* **2017**, *7*, 21484–21491. [CrossRef]

58. Murray, A.J.; Love, J.; Redwood, M.D.; Orozco, R.L.; Tennant, R.K.; Woodhall, F.; Goodridge, A.; Macaskie, L.E. Chapter 9: Enhancement of photosynthetic productivity by quantum dots application. In *Nonmagnetic and Magnetic Quantum Dots*; Stavrou, V.N., Ed.; InTech Publications: Rijeka, Croatia, 2018; pp. 147–174. [CrossRef]

59. Hu, L.; Tang, X.; Xu, J.; Wu, Z.; Lin, L.; Liu, S. Selective transformation of 5-hydroxymethyl furfural into the liquid fuel 2,5-dimethylfuran over carbon-supported ruthenium catalyst. *Ind. Eng. Chem. Res.* **2014**, *53*, 3056–3064. [CrossRef]

60. Roque, R.M.N.; Baig, M.N.; Leeke, G.A.; Bowra, S.S.; Santos, R.C.D. Study on sub-critical water mediated hydrolysis of Miscanthus a lignocellulosic biomass. *Resour. Conserv. Recycl.* **2012**, *59*, 43–46. [CrossRef]

61. Pasquini, D.; Pimenta, M.T.B.; Ferreira, L.H.; Curvelo, A.A.S. Extraction of lignin from sugar cane bagasse and *Pinus taeda* wood chips using ethanol–water mixtures and carbon dioxide at high pressures. *J. Supercrit. Fluids* **2005**, *36*, 31–39. [CrossRef]

62. Miao, Z.; Grift, T.E.; Hansen, A.C.; Ting, K.C. Energy requirement for comminution of biomass in relation to article physical properties. *Ind. Crops Prod.* **2011**, *33*, 508–513. [CrossRef]

63. Toledano, A.; García, A.; Mondragon, I.; Labidi, J. Lignin separation and fractionation by ultrafiltration. *Sep. Purif. Technol.* **2010**, *71*, 38–43. [CrossRef]

64. Mahant, B.; Linga, P.; Kumar, R. Hydrogen economy and role of Hythane as a bridging solution: A perspective review. *Energy Fuels* **2021**, *35*, 15424–15454. [CrossRef]

65. Ringoot, D.; Kleiven, H.; Panter, K. Energy efficient thermal hydrolysis with steam explosion. In Proceedings of the 17th European Biosolids and Organic Resources Conference, Leeds, UK, 19–21 November 2012.

66. Kepp, U.; Machenbach, I.; Weisz, N.; Solheim, O.E. Enhanced stabilisation of sewage sludge through thermal hydrolysis—Three years' experience with full scale plant. *Water Sci. Technol.* **2000**, *42*, 89–96. [CrossRef]

67. Penfold, D.W.; Redwood, M.D.; Yong, P.; Stratton-Campbell, D.; Skibar, W.; Macaskie, L.E. Microbial hydrogen and electricity from wastes. In Proceedings of the 7th Hydrogen-Power and Theoretical Engineering Solutions (HyPoThESIS VII), Merida, Mexico, 2007; ISBN 968-6114-21-1.

68. Sakr, M.; Liu, S. A Comprehensive review on applications of ohmic heating. *Renew. Sustain. Energy Rev.* **2014**, *39*, 262–269. [CrossRef]

69. Delbecq, F.; Wang, Y.; Muralidhara, K.E.; Ouardi, G.; Marlair, G.; Lin, C. Hydrolysis of hemicellulose and derivatives—A review of recent advances in the production of furfural. *Front. Chem.* **2018**, *6*. [CrossRef] [PubMed]

70. Shen, G.; Andrioletti, B.; Queneau, Y. Furfural and 5-(hydroxymethyl) furfural: Two pivotal intermediates for bio-based chemistry. *Curr. Opin. Green Sustain. Chem.* **2020**, *26*, 100384. [CrossRef]

71. Silva, J.F.L.; Mariano, A.P.; Filho, R.M. Economic production of 2-methyl tetrahydrofuran (MTHF) and ethyl levulinate (EL) produced from hemicellulose-derived furfural. *Biomass Bioenergy* **2018**, *119*, 492–502. [CrossRef]

72. Murray, A.J.; Zhu, J.; Wood, J.; Macaskie, L.E. Biorefining of platinum group metals from model waste solutions into catalytically active bimetallic nanoparticles. *Microb. Biotechnol.* **2018**, *11*, 359–368. [CrossRef]

73. Deplanche, K.; Merroun, M.L.; Casadesus, M.; Tran, D.T.; Mikheenko, I.P.; Bennett, J.A.; Zhu, J.; Jones, I.P.; Attard, G.A.; Selenska-Pobell, S.; et al. Microbial synthesis of core/shell gold/palladium nanoparticles for applications in green chemistry. *J. R. Soc. Interface* **2012**, *9*, 1705–1712. [CrossRef]

74. Nishimura, S.; Ikeda, N.; Ebitani, K. Selective hydrogenation of biomass derived 5-hydroxymethyl furfural (HMF) to 2,5-dimethyl furan (DMF) under atmospheric hydrogen pressure over carbon supported PdAu bimetallic catalyst. *Catal. Today* **2014**, *232*, 89–98. [CrossRef]

75. Beauregard, D.A.; Yong, P.; Macaskie, L.E.; Johns, M.L. Use of non-invasive magnetic resonance imaging to assess the reduction of Cr(VI) using a biofilm-palladium catalyst. *Biotechnol. Bioeng.* **2010**, *107*, 11–20. [CrossRef]

76. Yong, P.; Liu, W.; Zhang, Z.; Beauregard, D.; Johns, M.L.; Macaskie, L.E. One step bioconversion of waste precious metals into Serratia biofilm-immobilised catalyst for Cr(VI) reduction. *Biotechnol. Letts.* **2015**, *37*, 2181–2191. [CrossRef] [PubMed]

77. Orsi, E.; Beekwilder, J.; Eggink, G.; Kengen, S.W.M.; Weusthuis, A. The transition of *Rhodobacter sphaeroides* into a microbial cell factory. *Biotechnol. Bioeng.* **2021**, *118*, 521–541. [CrossRef] [PubMed]

78. Deilami, S. Advanced Studies of Catalytic Upgrading of Heavy Oil and Pyrolysis Bio-Oil. Ph.D. Thesis, University of Birmingham, Birmingham, UK, 2019.

79. Lee, S.Y.; Sankaran, R.; Chew, K.W.; Tan, C.H.; Krishnamoorthy, R.; Chu, D.-T.; Show, P.-L. Waste to bioenergy: A review on the recent conversion technologies. *BMC Energy* **2019**, *1*, 4–26. [CrossRef]

80. Zhang, Z.-H.; Sun, Z.; Yuan, T.-Q. Recent Advances in the catalytic upgrading of biomass platform chemicals via hydrotalcite-derived metal catalysts. *Trans. Tianjin Univ.* **2021**, *28*, 89–111. [CrossRef]